

Materials degradation in non-thermal plasma generators by corona discharge

Mar Cogollo (✉ mmar.cogollo@upm.es)

Universidad Politécnica de Madrid

Adrián López Arrabal

Universidad Politécnica de Madrid

Andrés Díaz Lantada

Universidad Politécnica de Madrid

M. Vega Aguirre

Universidad Politécnica de Madrid

Research Article

Keywords: corona discharge, corrosion, electrodes, non-thermal plasma, tungsten, nichrome, stainless steel, industrial application, lifespan, reliability

Posted Date: April 9th, 2021

DOI: <https://doi.org/10.21203/rs.3.rs-395613/v1>

License: © ⓘ This work is licensed under a Creative Commons Attribution 4.0 International License.

[Read Full License](#)

Materials degradation in non-thermal plasma generators by corona discharge

Mar Cogollo^{1,2}, Adrián López Arrabal¹, Andrés Díaz Lantada¹, M. V. Aguirre^{3,4}*

¹ Product Development Laboratory, Department of Mechanical Engineering, Escuela Técnica Superior de Ingenieros Industriales, Universidad Politécnica de Madrid, c/José Gutiérrez Abascal, 2, 28006, Madrid, Spain

² Research & Development Department, Cedrón, Consultoría Técnica e Ingeniería S.L, 28919 Leganés, Spain

³ Department of Aerospace Materials and Production, Escuela Técnica Superior de Ingeniería Aeronáutica y del Espacio, Universidad Politécnica de Madrid, 28040, Madrid, Spain

⁴ Centro de Investigación de Materiales Estructurales (CIME)

* Correspondence: mmar.cogollo@upm.es ; Tel.: +34-674-522-264

Abstract

Atmospheric corona discharge devices are being studied as innovative systems for cooling, sterilization and propulsion, in several industrial fields, from robotics to medical devices, from drones to space applications. However, their industrial scale implementation still requires additional understanding of several complex phenomena, such as corrosion, degradation and fatigue behaviour, which may affect final system performance. This study focuses on the corrosive behaviour of wires that perform as a high-voltage electrode subject to DC positive corona discharge in atmospheric air. The experiments demonstrate that the non-thermal plasma process promotes the growth of the oxidative films and modifies the physicochemical properties of the materials chosen as corona electrodes, hence affecting device operation. Surfaces exposed to this non-thermal plasma are electrically characterized by negative exponential decay of time-depend power and analysed with SEM. Implications on performance are analysed and discussed.

Keywords: corona discharge, corrosion, electrodes, non-thermal plasma, tungsten, nichrome, stainless steel, industrial application, lifespan, reliability

1. Introduction

Cold plasma technology has been recently researched and its potentials validated, through functional prototypes, for a wide set of industrial applications including innovative refrigeration systems [1-3], bacterial inactivation processes [4,5], surface treatment procedures and many others [6-8]. There are several configurations [9-11] that have been studied for the creation of related devices, capable of applying cold plasma to different industrial fields, from robotics to medical devices, from drones to space appliances. However, most available demonstrators are still in a prototype stage and little attention has been paid to long-term reliability, which is fundamental for increased safety, better operational stability, extended useful life and overall industrial and commercial success.

Continued use of corona discharge cooling devices in atmospheric air causes destructive and irreversible effects on the corona and ground electrodes. The environment where the discharge originates is considered an aggressive environment, as it is a highly oxidative medium. In the case of positive polarity, this is due to the presence of electrons that are directed towards the high voltage electrode, causing small shocks on its surface. On the other hand, the collector electrode is bombarded by chemical species such as O₃, NO_x and SO_x, which are generated during electrical discharge [12-15]. All these collisions of particles on the surface cause the activation of corrosion phenomena dependent on the exposure time and functioning conditions. The variation of the experimental and environmental conditions causes changes in the global power and overall performance of the device. Conditions such as local humidity, ambient temperature, ionization medium, applied voltage or degradation of the electrodes, can affect device stability by producing continuous electric arcs, hence causing a non-uniform discharge [16-18]. Because of different aforementioned variables, thin insulating layers may be generated during the use of these devices, which typically ends up with a smaller active area upon both electrodes. Progressively, the electrodes begin to lose their mechanical and electrical properties and the corona discharge efficiency is reduced. Materials selection and adequate management of degradation and corrosion phenomena plays, hence, a vital role.

Numerous investigations have focused on studying the erosion instigated by electrodes subjected to electric discharges with a high current density, point heating due to the presence of electric arcs and high applied voltage [19-21]. Under these conditions, micro-explosions are originated, due to a local concentration of high energy and overheating of the metal (leading to ecton production [21,22]). The initiation of these small explosions of metallic particles and the massive emission of electrons (generation of ecton) are decisive in the formation of oxidizing compounds. However, studies dealing with the degradation of surfaces exposed to positive and negative corona discharge are not common. In some investigations focused on corona discharge, the initial generation of an ecton is observed in the initial stage of the discharge, regardless of the polarity. Needle erosion has been studied, using typically copper cathodes in negative corona discharge applying Trichel pulses in atmospheric air for various configurations [23,24]. Nanometric craters appearing at the cathode needle have been reported, which indicates degradation of the electrode by an explosion emission mechanism. The value of the current density — $5 \cdot 10^8$ A/cm² — and the integral of the specific current action — $4 \cdot 10^9$ A²·s /cm⁴ — of the Trichel pulse allow for an explanation about the reason for the erosion of the cathode, which appears

to be originated by micro-explosions. Other tungsten, platinum, copper and lead electrodes have been studied, in negative corona discharges, with point-to-plane configuration and using an electrode gap of 3.1 cm in pure N₂ and H₂^[25]. With a current density of 1 A/cm², Weissler has reported the formation of craters, due to the mechanism of ecton erosion, as a consequence of the appearance of accumulated metal on the sides of the rounded tip.

In the case of positive corona discharge, there is much less information available, and the complex (and probably interwoven) corrosion mechanisms of the anode are still under debate. Recently, some authors have focused their research on understanding the reliability of wires as anodes ^[26-27]. Islamov and Krishtafovich have investigated the lifetime of the wires of different materials as a corona electrode. Tungsten, Au-coated stainless steels, Ni-Cr alloys and silver alloys have been explored. Nichrome and silver and their alloys appear to present a very high average erosion rate, which limits their use to approximately 50 to 100 hours (h). The most promising results have been described for tungsten and gold wires, which achieve lifetime of even some months. Comparing both materials, tungsten has a lower average anodic erosion rate than gold wires, being 0.24 µg/C and 0.60 µg/C, respectively. Finally, the trendline of the erosion rate of the wolfram filament presents an exponential model ($S_w [\mu\text{g}/\text{C}] = (0.20 \pm 0.10) \cdot \exp(0.011 \pm 0.020 \cdot Q)$). Considering the information available in the literature, the beginning of an analysis is proposed, in order to determine the optimal electrode for future implementation on an industrial scale.

In this research, the main objective is to analyze the erosion generated during the ionization process and, consequently, improve the reliability of an industrial electrohydrodynamic (EHD) cooling system. The system corresponds to the “TRAID” arrangement, presented in previous studies by our team ^[3,28]. Present study focuses on systematically evaluating the use of diverse wires as corona electrodes for DC positive corona discharge in atmospheric air and takes into consideration different diameters and materials. Tungsten, nichrome and stainless steel are considered due to their properties and potential for reliable and profitable performance in EHD cooling systems. The time-dependent power loss, related to electrical resistance, is measured to determine the rate of erosion, to predict the rate of corrosion and as a variable linked to overall performance and useful device life.

Furthermore, to understand the degradation process and the underlying mechanisms, electrodes exposed to discharge at different times are visualized by scanning electron microscopy (SEM), which leads to discovering varied corrosion mechanisms that affect corona discharge systems. Materials and methods employed are detailed below, before presenting and discussing main results.

2. Materials and methods

This research has led to a comprehensive characterization of the TRAIID configuration, which is a specific electrode system shown schematically in Figure 1, performing as DC positive corona discharge system. The experimental electrohydrodynamic (EHD) pump follows a U-geometry and the corona electrode is made up of a wire fixed to the U-collector electrode at determined distance known as gap. First of all, the device is electrically characterized to record the loss of power over time. Subsequently, after corona discharge, a methodic study of filaments is performed by means of scanning electron microscopy (*Mitsubishi S-3400N SEM system*). All experiments are carried out at atmospheric pressure and ambient temperature (20-25 °C).

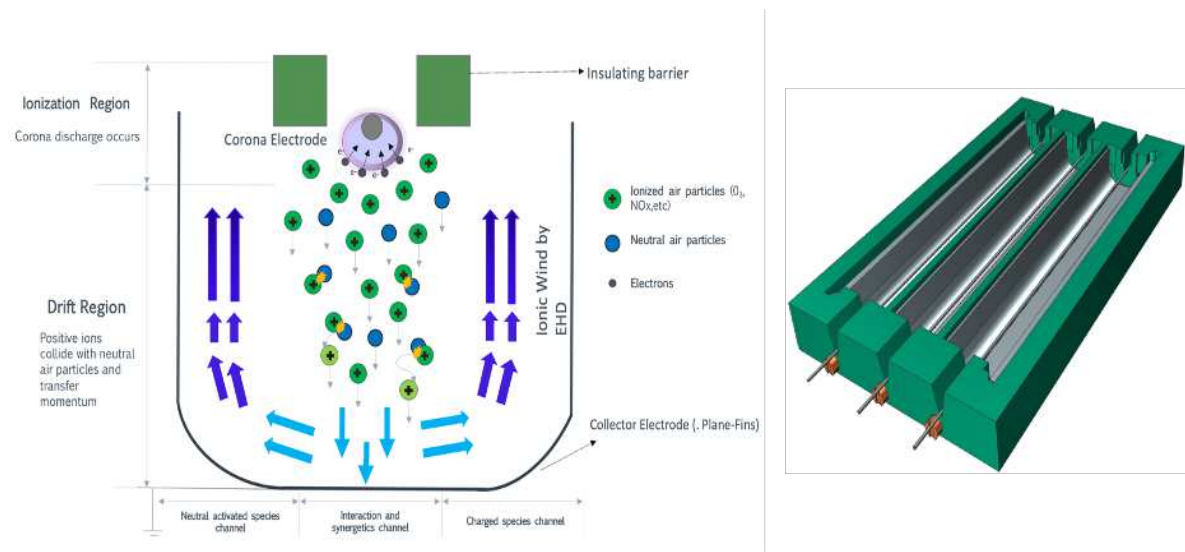


Figure 1. Schematic diagram of positive corona discharge and CAD design of TRAIID configuration.

2.1 Experimental set-up

The configuration studied in Figure 1 can be tested by using a device that has been designed with the help of the NX-8.5, which is commercial computer-aided design and engineering software by Siemens PLM Solutions. The manufacturing of the prototype is carried out using a fused deposition modeling 3D printer, with commercial denomination Sigma R19 BCN3D. The device structure is made of polylactic acid (PLA) 850 filament and is used to hold both electrodes at a fixed distance. The device studied consists of two pieces which are assembled: the corona support and the metallic bulk ground plate with fins.

The different corona wire electrode materials include tungsten (W 99.95%), stainless steel (S30200) and nichrome ($\text{Ni}_{0.8}\text{Cr}_{0.2}$). The wires measure 40 mm in length and diameters of 25, 50 y 100 μm are analysed, at an electrode gap of 2 mm from the U-collector aluminium (Al alloy- 7075) electrode. The U-collector electrode dimensions consist of an internal channel with a width of 8 mm and counts fins with a height of 6 mm. The corona wire electrode is set at the same distance from both fins.

2.2.- Performance evaluation

To study the wear or degradation of the different electrode materials and to obtain the erosion rates for each case, different device structures with the same geometry and parameters are needed and tested. Corona experiments are performed to study the response, performance and stability of different materials during the positive electric discharge phenomenon. The current-voltage characteristic curves (CVCs) are studied for different times of exposure at a constant voltage. Consequently, the power and electrical wire resistance respect to time are obtained and studied. In this way, the impact of electrode erosion on the behaviour of the EHD system can be verified. The corona equipment used in this research includes a high voltage power supply Heinzinger LNC 10,000-5, where both electrodes are connected for positive DC discharge up to 6 kV, which produces a potential difference between the corona wire electrode and the collector electrode. The wire power is monitored using a data logger RS PRO TES-1384 and a digital multimeter FLUKE 115 TRUE RMS. Due to the micrometric sizes of the high voltage electrode, determining the components of the oxidized film and its thickness using chemical analysis and visualization techniques is a challenge. The studies of the surface for different materials, used as electrodes, are performed both before and after the corona treatment through SEM microanalyses.

3. Results and discussion

3.1.- Power – time measurements

Tests are performed to determine the behaviour of different corona electrodes materials exposed, during relevant amounts of time, to positive corona discharge at high voltages typical from real operation. Under the corona discharge effect, the thermophysical properties of electrode materials play an essential role in erosion. Tungsten (W), nichrome (NiCr) and stainless steel (SS) are evaluated as potentially interesting materials to develop the experiments, because they are electrically conductive, have good corrosion resistance and are commercially available. In the experiments presented, the wires used as corona electrodes have the 40 cm in length and the diameters vary between 25, 50 or 100 μm . Current-voltage characteristics curves are determined for different times of exposure at a fix voltage. This voltage typically depends on the geometric parameters of the device: distance between electrodes, wire diameter and configuration. As time increases, the current decreases; as a result, higher values for operating voltages are required, which reduces the performance and life span of the devices.

Based on the different values obtained by the CVCs curves the power consumption for the different materials is determined. As the exposure time to the corona discharge effect is increased, the corona power decreases. The experiments stop when the break point of the wire is reached or when the number of sparks forms a continuous stream that creates a short circuit. To be able to compare the behaviour for each wire, an almost fixed operating voltage that varies in a range of 4 to 5.2 kV is established. All filaments are tested from 1 to 1.5 W of initial power.

To evaluate the different materials used as corona electrodes, a first round of experiments is performed using a 50-micron wire diameter for all of them. All curves represented in *Figure 2* are an average of the tests performed for each wire, in order to analyse power loss with increasing exposure of the devices to the corona discharge. For the 50 μm diameter wires both experiments of stainless steel and nichrome are stopped, as they break at 50 and 95 hours, respectively. Tungsten wire does not break but the streamers formed

make impossible the study when the 200 hours are reached. We can observe how Ni-Cr and W wires have similar behaviour for the first 70 hours which they only arrive at a power loss of 20%. After that point we can observe a drop of power for nichrome wire in its last 30 hours of lifetime.

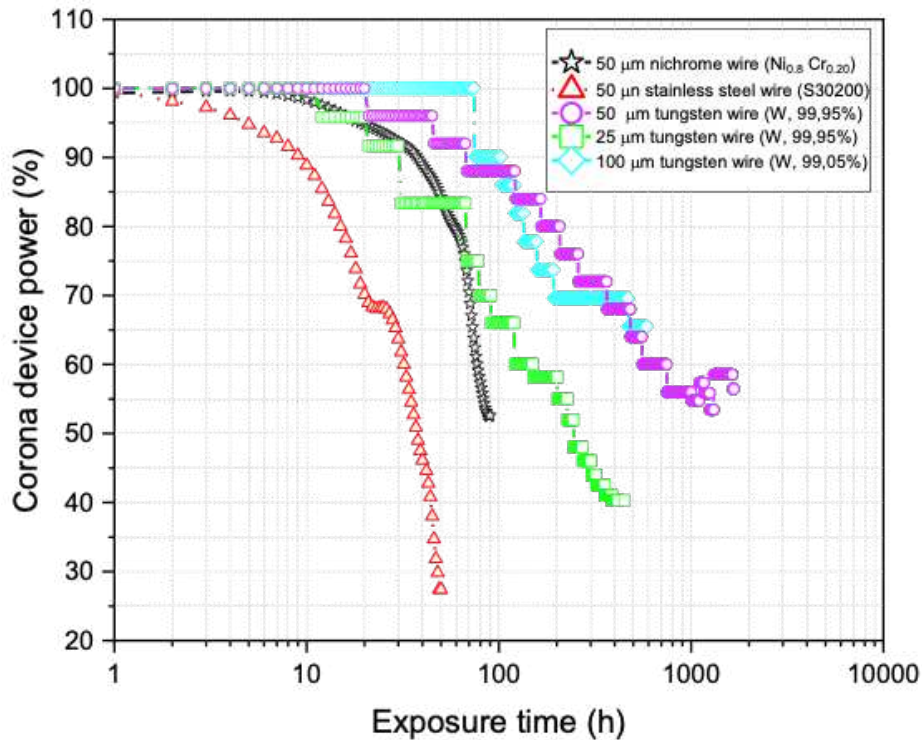


Figure 2. Power loss of different electrode wires under positive high voltage corona discharge.

Stainless steel is considered to have a bad response to corona power consumption, as it breaks soon with a high-power drop. Comparing all different materials for the same diameter, tungsten wire exhibits a better performance, as the wire does not break during any of the performed experiments and because it leads to the lowest values for the corona power reduction. Subsequently, a second round of experiments is performed with tungsten wires and with varying diameters of 25 and 100 microns, in order to determine the useful life of these electrodes for its industrialization. As shown in *Figure 2*, the tungsten with different diameter sizes presents a similar power drop around 60 hours of use for all studies. Regarding the 25-micron wire diameter, when its power drops by up to 40%, it stabilizes for up to 450 hours, when continuous arcs or streamers begin to form. On the other hand, the 50- and 100- micron corona electrodes stabilize after an exposure of approximately 200 hours up to service times exceeding 1,000 hours. In these last two cases, the tests are stopped to visualize them by scanning electron microscopy.

3.2.- Degradation of W, Stainless steel 302 and Nichrome corona wires electrodes: Erosion rate (E)

Anode degradation is investigated in positive corona discharge in atmospheric air. The micro-craters produced by the ecton generation are related to the mechanism of erosion and oxidation in corona filaments. Investigation of anode degradation rate is developed for several different configurations shown in Table 1. Lifespan testing initiates with new W, Ni-Cr, and stainless steel (S30200) filaments of 50 μm . Nichrome and stainless-steel

wires show an increase in electrical resistance in a few hours of discharge exposure, causing breakage or streamer formation. The generation of a uniform oxide layer is macroscopically visible in both previous materials with an ash gray color in the initial 40 hours of testing. Regarding tungsten wire, in the first 80 hours there is no appreciable change for its operation. However, after this period of time, the resistance of the filament begins to increase slowly until stabilizing to 200 hours of procedure, when the gray-whitish generated oxidation layer is already visible. This behavior of the tungsten filament is verified for other sizes of 25 and 100 μm , respectively. Following the similar trend, an alteration in electrical resistance occurs within the first few hours but stabilizes over time until the electrical discharge is not uniform. For the TRAIID configuration, it can be determined that the service life of tungsten filaments exceeds 1,000 hours but with significant damage due to the corrosion mechanisms that these wires develop.

Table 1. Experimental considerations, materials and average degradation rate of W, Ni0,8Cr0,2 and stainless steel.

| Material | D (μm) | Number assays | ΔV (kV) | Exposure time, t_r (h) | Corona power reduction (%) | Final State | Final current, I ($\mu\text{A}/\text{cm}$) | Q_f (C/cm) | e_a ($\mu\text{g}/\text{C}$) |
|-------------------------------------|---------------------|---------------|-----------------|--------------------------|----------------------------|-------------|--|--------------|----------------------------------|
| Stainless steel 302 | 50 | 12 | 4.75 | 50 | 72.7 | Rupture | 15 | 4 | 29 |
| Ni _{0.8} Cr _{0.2} | 50 | 8 | 4.75 | 95 | 48 | Rupture | 32.5 | 11.1 | 7.6 |
| Tungsten | 50 | 18 | 4.5 - 4.75 | 1,630 | 56.5 | Stopped | 50 | 300.42 | 0.92 |
| | 25 | 8 | 4 - 4.3 | 450 | 40.3 | Stopped | 27.5 | 44.5 | 3.7 |
| | 100 | 10 | 4.9 - 5.2 | 600 | 65.2 | Stopped | 40 | 86.4 | 5.3 |

The erosion rate is a difficult parameter to estimate because numerous phenomena overlap during corona discharge. Several authors such as Islamov and Krishtafovich^[27] estimated the erosion rate of various materials in their configuration. They related to this physicochemical phenomenon with the volume of filament subjected to discharge, the intensity and the time of exposure. The average erosion rate formula e_a for a wire is expressed in $\mu\text{g} / \text{C}$ and is shown below:

$$e_a = \frac{1}{Q} \int_0^Q E dQ = \frac{\Delta m_a}{Q} = \frac{A_d}{Q} \cdot \left(1 - \frac{R_0}{R_a}\right) \quad (1)$$

where E is the global rate of erosion as a function of Q(t) which is the charge transferred per unit length of the cable in C/cm. The charge transferred per unit length is defined as $Q(t) = \int_0^t I dt$, where I is the current of the corona filament per unit length in $\mu\text{A}/\text{cm}$. On the other hand, A_d is the association with the cross section and the density of the electrode material, $A_d [\mu\text{g}/\text{cm}] = 10^6 \cdot \pi \cdot (r [\text{cm}])^2 \cdot \rho [\text{g}/\text{cm}^3]$; R_0 and R_a are, respectively, the initial and final values of the resistance per unit length of the electrode in the active exposure zone of the corona discharge. Estimating the erosion caused during the corona discharge process is a complicated method of determining when it depends on time. By improving the accuracy of this degradation rate, successive measurements can be used. It

is considered that the overall erosion rate is proportional to the derivative of the corona electrode resistance R_0/R in relation to the minority transferred charge Q .

$$E_{i+\frac{1}{2}} = \frac{A_d}{Q_{i+\frac{1}{2}}} \cdot \left(\frac{R_0}{R_i} - \frac{R_0}{R_{i+1}} \right) \quad (2)$$

As previously discussed, the erosion phenomenon of the corona anode is one of the main reasons why filament rupture occurs. In *Figure 3*, the worst degradation behavior of stainless steel is determined, presenting a rupture at $Q=3$ C/cm and an average erosion rate of $29 \mu\text{g}/\text{C}$. A similar behavior is shown by the nichrome electrode which has a limited useful life, breaking at a transferred charge of $16 \text{ C}/\text{cm}$. However, the tungsten electrode has an average erosion rate $1.9 \mu\text{g}/\text{C}$ that remains unaffected with the exposure time, being the lowest of all electrodes.

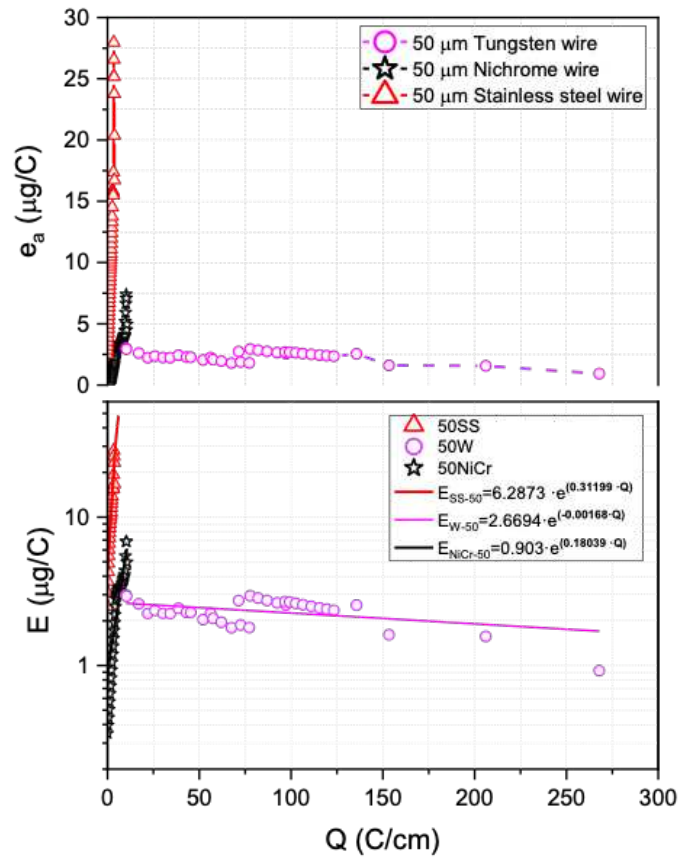


Figure 3. Analysis of tungsten, nichrome and stainless steel as corona electrodes relating average erosion rate (e_a) and erosion rate (E) depending on transferred charge. All corona electrode assays are shown in Table 1.

The erosion rate is approximated exponentially for all the cables studied. An exponential regression and interpolation model of all the data obtained by the data logger is created. The erosion rate for $50 \mu\text{m}$ tungsten, nichrome and stainless-steel filaments is determined considering the model fit errors and a coefficient of determination R^2 that is in a range from 0.61 to 0.88.

$$E_{SS-50}[\mu\text{g}/\text{C}] = (6.2873 \pm 2.06057) \cdot e^{(0.31199 \pm 0.09702 \cdot Q)}$$

$$E_{NiCr-50}[\mu\text{g}/\text{C}] = (0.90134 \pm 0.41284) \cdot e^{(0.18039 \pm 0.04647 \cdot Q)}$$

$$E_{W-50}[\mu\text{g/C}] = (2.6694 \pm 0.0928) \cdot e^{(-0.00168 \pm 0.0015 \cdot Q)}$$

The results of the average erosion rate for the different W wires studied dependent on the charge transfer are shown in *Figure 4*. It is observed that an average erosion rate for the W filament of 25 μm remains approximately 3.7 $\mu\text{g/C}$. On the other hand, the 50- and 100- μm anodes, unpredictably, do not have a similar average erosion rate in most of the tests performed. The 50-micron wire is remarkable because it has a low erosion rate compared to the other two wire sizes, being from 1.9 to 0.9 $\mu\text{g/C}$. Instead, the erosion rate performance for the three different diameters of tungsten shows a stable and constant trend when a charge transfer of about ~ 25 C/cm is exceeded. However, the erosion behavior of tungsten shows an appreciable difference with our electrode arrangement being higher than that reflected in the literature. These results may be associated with the prototype geometry and the different applied electrical parameters. For the TRAIID configuration it is estimated that it has an erosion rate exposed below:

$$E_w [\mu\text{g/C}] = (3.9854 \pm 0.1628) \cdot e^{(-0.000726 \pm 0.000052 \cdot Q)}$$

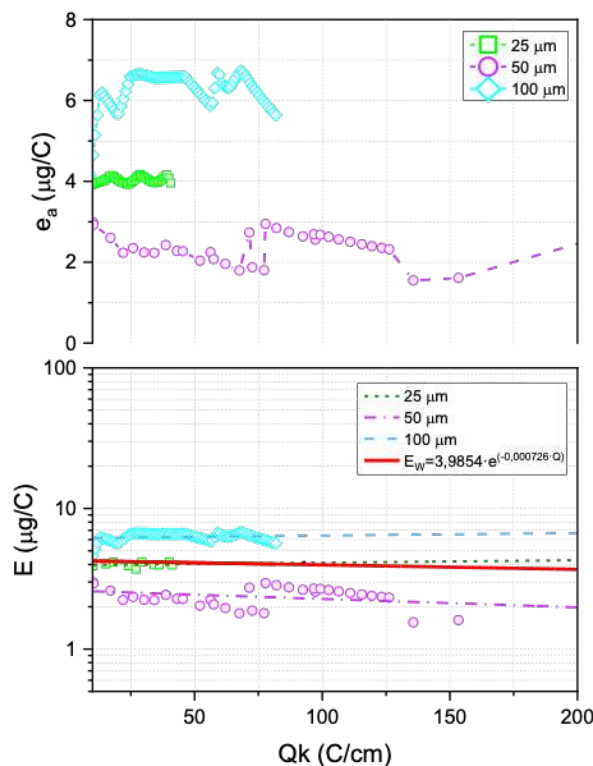


Figure 4. Average erosion rate and global erosion rate S depends on charge transferred per unit length Q considering different tungsten wire diameters.

In general, it is determined that nichrome and stainless steel are not competitive electrodes for use in non-thermal plasma in atmospheric air (for corona discharge applications) due to their accelerated corrosion and their limited-service life. On the other hand, tungsten is still the best material due to its refractory behavior and good resistance to degradation. However, due to the aggressive environment where the discharge has effect, the erosion and oxidation mechanisms are the main dominant phenomena that produce an electrode lifespan of 1,630 hours without cleaning and maintenance.

3.2.- Accelerated degradation under corona discharge phenomena

While studying the degradation of electrodes under corona discharge, it has been identified time as a critical factor. The amount of time needed to obtain consistent values for service life in electrodes could require years of tests. Due to this, the importance of accelerating the amount of damage generated on electrodes while being tested and being able to quantify that damage has been one of our goals.

The acceleration of time damage on electrodes has been done by calculating the cumulative energy density that the electrode handles in MJ/cm². By using that parameter, we can on one side, obtain typical values of cumulative energy density in which the electrode breaks and on the other side set a strategy to increase the energy density the electrode handles in each time step to reduce testing length.

The selection of energy density has been made since this energy has been proved to be the driving force of all the chemical reactions and therefore it directly influences service life [29]. Energy density has been chosen instead of energy because it's easier to scale it to different kind of electrodes by taking its surface as reference. Also, the exposed surface is the place where most of the reactions take place in between chemical elements, molecules, electrodes, etc.

The steps to calculate the energy density are shown in equations (4), (5) and (6).

$$W = I \cdot V \quad (4)$$

$$\rho_W = \frac{W}{S_c} \quad (5)$$

$$\rho_E = \frac{1}{10^6} \int_0^t \rho_W \cdot dt \quad (6)$$

Where W refers to power in [W], I refers to current in [mA], V refers to Voltage in kV, S_c refers to the electrode surface in cm², ρ_w refers to power density in W/cm² and ρ_E refers to energy density in MJ/cm².

Integrating equation (6), for the experiments done on the degradation benches, the results shown in Figure 5 are obtained.

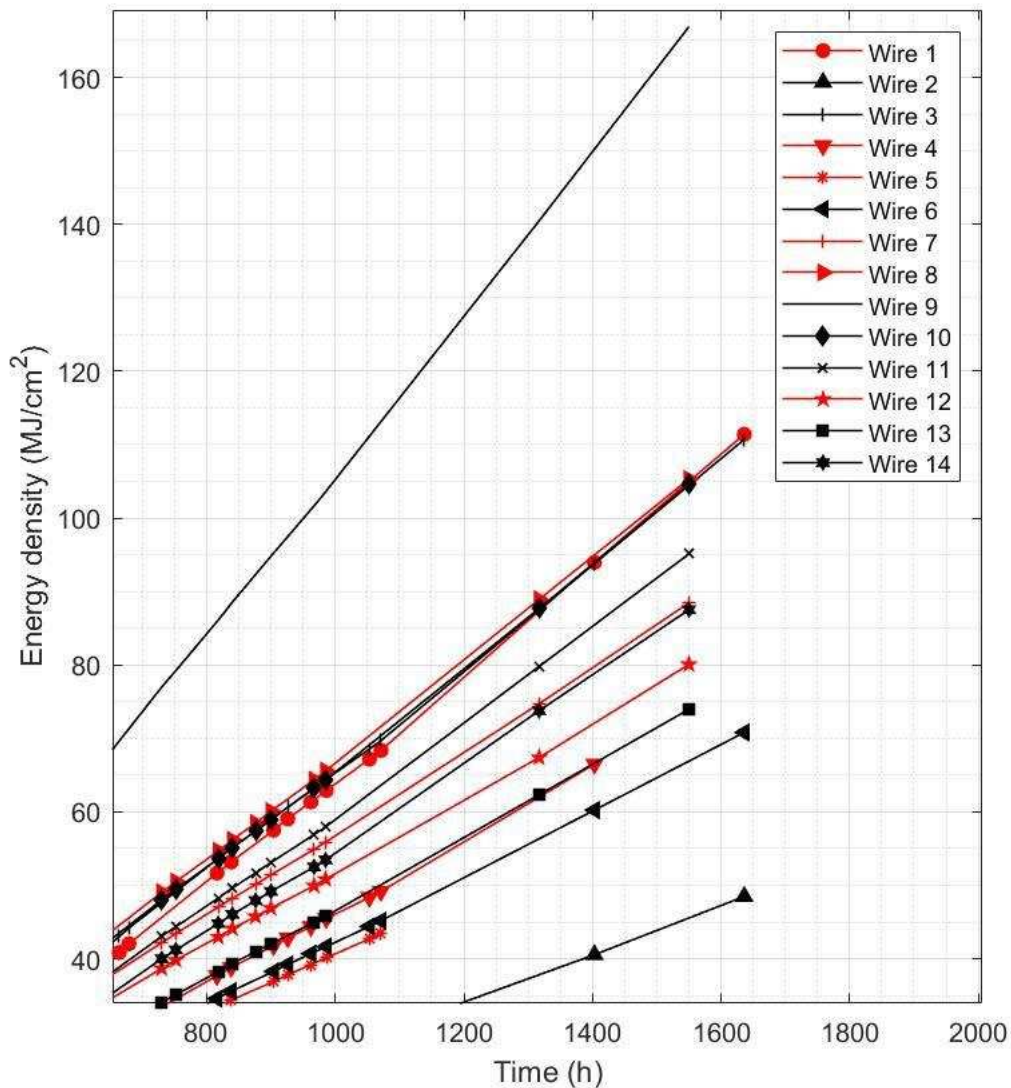


Figure 5. Cumulated energy density (MJ/cm^2) recorded for 14 wire electrodes tested for 1,550-1,630 hours.

These test benches have been studied at a higher service power to obtain the limit of accumulated energy density that an electrode can handle. At approximately 1,550 hours, the maximum value obtained is $166 \text{ MJ}/\text{cm}^2$.

With that cumulative energy density result and the power loss on electrodes we can give a rough service life estimation at designed operating condition for electrodes ^[30]. This result has been calculated for several power densities that can be seen in Figure 6 (in this case, we use linear power density in W/cm for design purposes).

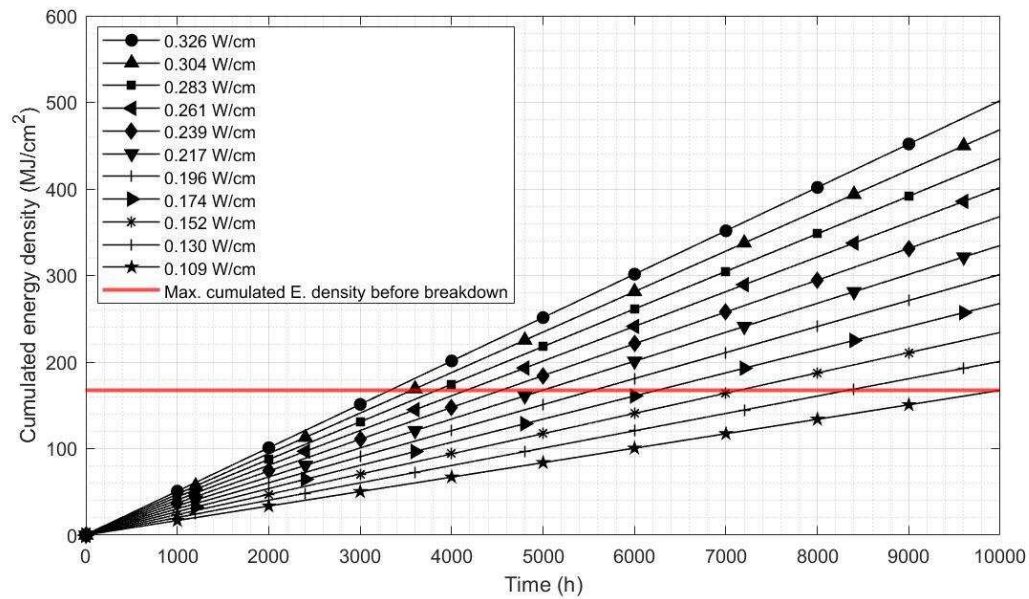


Figure 6. Service life prediction for different levels of power density on wire electrodes.

The horizontal red line represents the current cumulative energy density limit which grows while the time the test electrodes are exposed to high power grows. Right now, the estimated service life for electrodes at average power is 4,980 h. At minimum power it can be increased up to 10,000 h and at maximum power it decreases to 3,300 h.

To improve the reliability of this model and for being able to obtain a higher cumulative energy density limit in a shorter period of time, it is planned to accelerate even more the test by increasing the energy that the electrode handles. Several ways to increase that energy have been studied ^[31]. The easiest one is increasing the voltage in between electrodes but it can make the discharge less stable. That is why in the future tests will be done in other atmosphere with higher temperature and lower pressure to increase the energy density while keeping the discharge stable.

The aim of increasing the energy density is to reach an acceleration factor of more than 10 (predicted hours/tested hour), being this number right now is around 3,2.

3.3.- Surface morphology: SEM analysis before and after exposure corona discharge

Corona electrodes are analyzed using scanning electron microscope (SEM) images. The study of different diameters of tungsten wires are observed over the central length exposed to the corona discharge. First, the diameter tungsten wire of 25 μm for different hours is visualized obtaining images like the ones shown in *Figure 7*. Starting from a electrode wire without exposure to corona discharge (see *Figure 7a*), the advance of oxidation is observed, according to the formation of plasma with time, beginning to originate oxides in the surface not uniformly after 20 h (*Figure 7b*).

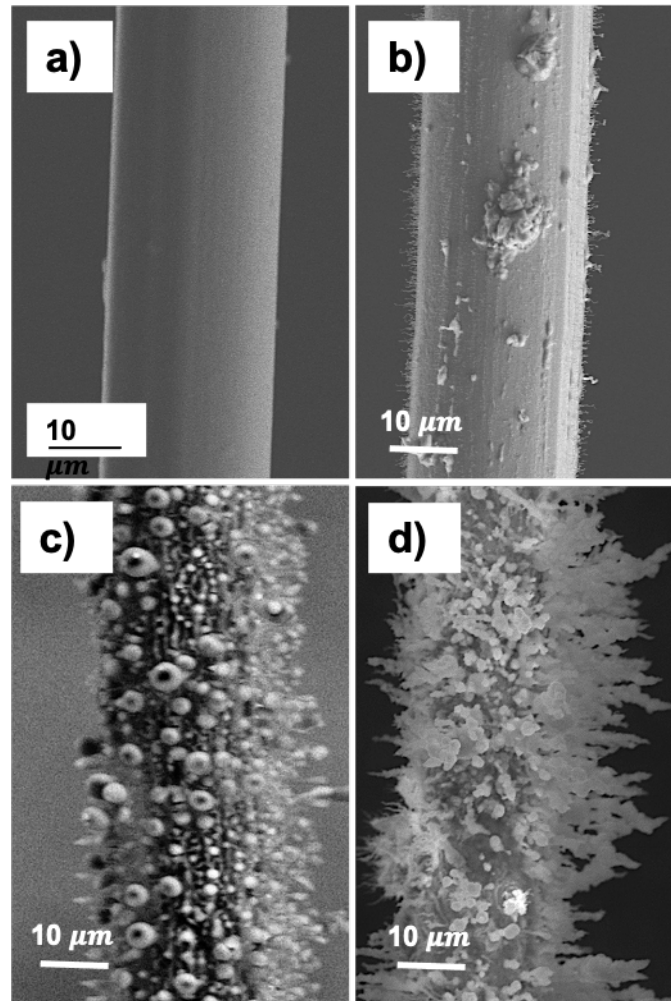


Figure 7. Tungsten wire of 25 μm exposed at a) 0 hours, b) 20 hours, c) 280 hours and d) 450 hours by atmospheric corona discharge.

Considering a longer exposure time, reaching up to 400 h of use, an irregular oxidative film based on spherical and fractal structures can be seen, mostly in the ionization zone, as shown in Figure 7c) and 7d). This corrosive phenomenon causes significant changes in the discharge as well as in the direction and intensity of the electric field due to the presence of this film, causing a smaller effective discharge area. As a consequence, electric arcs and streamers are created and are tried to go through the corroded film. It is important to consider that although this continuous formation of oxides due to erosion and the oxidative medium where it occurs is quite unstable and most of the oxides volatilize.

The tungsten anode of 50 and 100 μm after corona discharge is shown in Fig. 8. An oxide layer with a rough surface forms on the 50 μm filament after 250 hours of discharge over the entire surface of the anode (Figure 8a) and 8b). Two significant regions are shown: on the one hand, areas with stable oxide layers around the anode; on the other hand, sections affected by the impact of an arc which has caused the rust shell to break and local fusion in that area.

On the exposed surface in front of the ground electrode, nanometric craters are visualized at 40 and 185 h (see Figure 8c) and 8d)). Around these micro-explosions, nanometric oxides begin to form, overlapping several effects: local temperature changes due to the

impact of electrons with temperatures above 10,000 K, atmospheric air as a corona discharge medium that induces accelerated oxidation and the application of a high electric field that directly influences the degradation mechanism. An exposure time of 470 hours is evaluated in the SEM images (Fig. 8e) and 8f) in which two significant regions are also observed where the oxide presents a uniform velvet pattern and fused areas that cause discontinuities in the discharge.

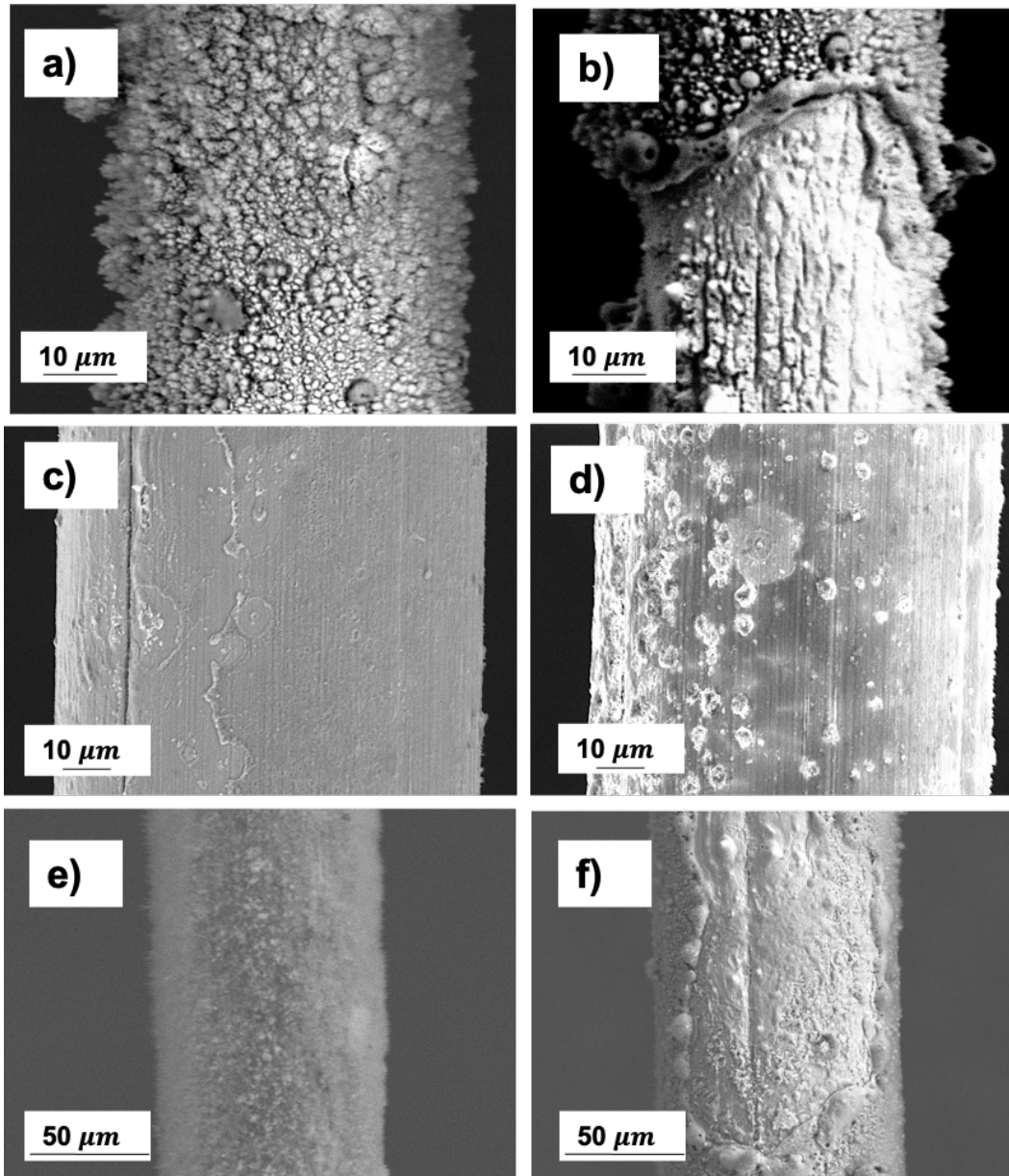


Figure 8. Tungsten filament of 50 μm after treatment at a) and b) 250 hours which a dense and non-uniform oxidation layer can be observed on the entire external surface, observing in some areas the rupture of the oxide layer due to the instability of the discharge. In the micrographs c) and d), the 100 microns tungsten anode is visualized at different exposure hours, 40, 180 hours respectively, where bombardments begin to occur by the electrons. e) and f) SEM images showing W filament of 100 μm undergoes a corona discharge at 470 hours, showing stable layer of oxides with a pattern similar to velvet and fused areas due to the generation of punctual micro-arcs.

In addition to the oxidation film created, electron bombardment-induced erosion results in significant mass loss over time. It can be clearly seen how the wire in a certain area experiences a considerable decrease in the cross-sectional area (see Figure 9). This could

be because of combination of the localized losses of oxide layers, due to microarcs produced, and plastic deformation promoted by the operating temperature during these phenomena. The Ductile-Brittle Transition Temperature (DBTT) of tungsten is in the interval of 200-450 °C [32,33], but it depends on metallurgical factors that can do it to change. Plastic deformation in tungsten only is possible if the temperature is over this DBTT. Therefore, the reached temperature in these areas has been higher than the transition temperature. This change in dimensions directly influences the operation of the discharge, this area being a critical point of electrode breakage. The presence of longitudinal cracks can be caused by the wire manufacturing process and the excessive tension applied to fix the filament on the prototype. These structural imperfections also influence corrosion, accelerating the entire process.

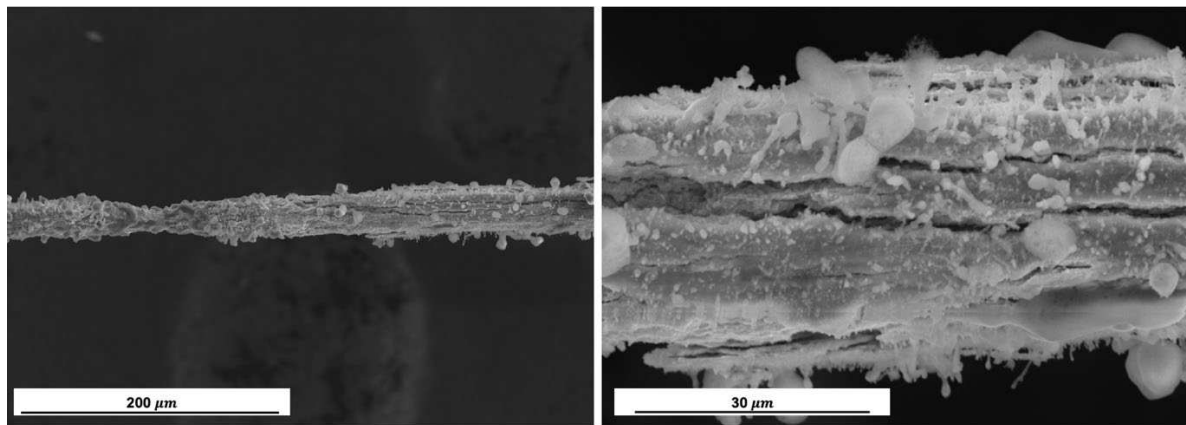


Figure 9. Thickness change of W wire of 25 μm after 300 hours in service due to erosion and corrosion triggered in the process. There is a reduction in section that may be due to the combination of localized detachment by micro-arcs. Also due to plastic deformation favored by focused temperature increases in specific arc-areas. Necking has been observed in some filaments without appreciable degradation.

4. Conclusions and perspectives

The industrial success of atmospheric non-thermal plasma devices relies on adequately taking the deterioration of active electrodes into account. In this study, the degradation of the surfaces of corona electrodes has been demonstrated for most materials used as active electrodes in ionic wind generation devices. For most materials, this degradation starts after a short period of use, which importantly limits electrode life. A superposition of corrosive effects such as the impact of electrons on the surface at high temperatures and atmospheric air as a means of ionization cause accelerated corrosion in the vicinity of the wire. This corrosion leads to misshapen and non-uniform structures along the plasma exposed wire. Numerous materials are studied as active electrodes. Nichrome, stainless steel and tungsten of 50 μm are tested with the same configuration and power to estimate their useful lifetime in non-thermal plasma devices. The power loss of more than 50 % in nichrome and stainless steel is verified after 50 hours, causing the breakage of the wire in most of the tests carried out.

Therefore, tungsten is studied for different wire sizes (25, 50 and 100 μm) where its loss of properties after corona discharge is evaluated for several hours. The W filament can be used for approximately 1,000 hours with a loss of power less than 60% in the wires which are analysed. The aim is based on determining the total service life thought an energy model related to the power of the device is proposed. With the experimental tests carried

out, they allow us to determine an approximation of 4,980 hours of operation for high powers. However, a low power density of the device allows us to ensure a lifespan of more than 10,000 hours, being competitive with other industrial methods.

According to our experiments, tungsten is one of the corona electrodes with the greatest potential for industrialization according to our research and other authors who determine its possible use. It is important to highlight that the key to success of corona discharge electrode materials is, not only related to the capability of withstanding the discharge in service, but also to their processability and cost. Although tungsten provides the best compromise among the material studied, corona discharge systems are not yet competitive, in terms of lifespan, when compared to other conventional refrigeration systems.

However, corona discharge cooling devices present important advantages in terms of size, weight and ease of operation, which motivates further studies linked to achieving a deeper understanding of electrode degradation phenomena and to micro and nanomanufacturing post processes for improving the electrode endurance to corrosion. For all these reasons, and considering the aforementioned advantages of ionic wind devices, the most important challenge is to increase the service life of the electrodes.

Acknowledgments: This research work was supported by CEDRION C.T.I. S.L, Consejería de Investigación y Educación (Programa de Doctorados Industriales, Comunidad Autónoma de Madrid) through industrial doctoral scholarship IND2017/IND-7799 with Technical University of Madrid and grants by the Community of Madrid for entrepreneurial companies (S-2018\L2-95, RIS3).

References

- [1] Elagin, I. A., Yakovlev, V. V., Ashikhmin, I. A. & Stishkov, Y. K. Experimental investigation of cooling of a plate by ionic wind from a corona-forming wire electrode. *Tech. Phys.* (2016). doi:10.1134/S1063784216080077
- [2] Baudin, N., McEvoy, J., Rouzes, M., Persoons, T. & Robinson, A. J. Experimental investigation of ionic wind cooling in plate fin heatsinks and needle electrode arrangements. in *InterSociety Conference on Thermal and Thermomechanical Phenomena in Electronic Systems, ITherm* (2019). doi:10.1109/ITHERM.2019.8757423
- [3] Cogollo, M., Balsalobre, P. M., Lantada, A. D. & Puago, H. Design and experimental evaluation of innovative wire-to-plane fins' configuration for atmosphere corona-discharge cooling devices. *Appl. Sci.* (2020). doi:10.3390/app10031010
- [4] Sakudo, A., Yagyu, Y. & Onodera, T. Disinfection and sterilization using plasma technology: Fundamentals and future perspectives for biological applications. *International Journal of Molecular Sciences* (2019). doi:10.3390/ijms20205216
- [5] Kaci, M. et al. Investigation on the Corona Discharge in Blade-to-Plane Electrode Configuration. *Brazilian Journal of Physics* (2015). doi:10.1007/s13538-015-0357-4

- [6] Kim, J. S. *et al.* Particle removal characteristics of a high-velocity electrostatic mist eliminator. *Aerosol Air Qual. Res.* (2020). doi:10.4209/aaqr.2019.12.0648
- [7] Rezaei, F. *et al.* Investigation of plasma-induced chemistry in organic solutions for enhanced electrospun PLA nanofibers. *Plasma Process. Polym.* (2018). doi:10.1002/ppap.201700226
- [8] Boelter, K. J. & Davidson, J. H. Ozone generation by indoor, electrostatic air cleaners. *Aerosol Sci. Technol.* (1997). doi:10.1080/02786829708965505
- [9] Kasdi, A. Computation and measurement of corona current density and V–I characteristics in wires-to-plates electrostatic precipitator. *Journal of Electrostatics* (2016). doi: 10.1016/j.elstat.2016.02.005
- [10] Zhao, P., Portugal, S. & Roy, S. Efficient needle plasma actuators for flow control and surface cooling. *Appl. Phys. Lett.* (2015). doi:10.1063/1.4927051
- [11] Kaci, M. *et al.* Investigation on the Corona Discharge in Blade-to-Plane Electrode Configuration. *Brazilian Journal of Physics* (2015). doi:10.1007/s13538-015-0357-4
- [12] Nashimoto, K. Effect of electrode materials on O₃ and NO_x emissions by corona discharging. *J. imaging Sci.* (1988).
- [13] Goldman, M., Goldman, A. & Sigmond, R. S. The corona discharge, its properties and specific uses. *Pure Appl. Chem.* (1985). doi:10.1351/pac198557091353
- [14] Johnson, M. J. & Go, D. B. Recent advances in electrohydrodynamic pumps operated by ionic winds: A review. *Plasma Sources Science and Technology* (2017). doi:10.1088/1361-6595/aa88e7
- [15] Chen, J. & Davidson, J. H. Ozone Production in the Positive DC Corona Discharge: Model and Comparison to Experiments. *Plasma Chem. Plasma Process.* (2002). doi:10.1023/A:1021315412208
- [16] Yan, P. *et al.* An experimental study on the effects of temperature and pressure on negative corona discharge in high-temperature ESPs. *Appl. Energy* (2016). doi:10.1016/j.apenergy.2015.11.040
- [17] Reuter, S. *et al.* The Influence of Feed Gas Humidity Versus Ambient Humidity on Atmospheric Pressure Plasma Jet-Effluent Chemistry and Skin Cell Viability. *IEEE Trans. Plasma Sci.* (2015). doi:10.1109/TPS.2014.2361921
- [18] Ono, R., Teramoto, Y. & Oda, T. Effect of humidity on gas temperature in the afterglow of pulsed positive corona discharge. *Plasma Sources Sci. Technol.* (2010). doi:10.1088/0963-0252/19/1/015009
- [19] Puchkarev, V. F. & Bochkarev, M. B. High current density spotless vacuum arc as a glow discharge. *IEEE Trans. Plasma Sci.* (1997). doi:10.1109/27.640670

- [20] G.J.J. Winands, Z. Liu, A.J.M. Pemen, E.J.M. Van Heesch, K. Yan, *Rev. Sci. Instrum.* **2005**. 1. Winands, G. J. J., Liu, Z., Pemen, A. J. M., Van Heesch, E. J. M. & Yan, K. Long lifetime, triggered, spark-gap switch for repetitive pulsed power applications. *Rev. Sci. Instrum.* (2005). doi:10.1063/1.2008047
- [21] Mesyats, G. A. Ecton or electron avalanche from metal. *Uspekhi Fiz. Nauk* (1995). doi:10.3367/ufnr.0165.199506a.0601
- [22] Mesyats, G. A. Ectons and their role in plasma processes. in *Plasma Physics and Controlled Fusion* (2005). doi:10.1088/0741-3335/47/5A/010
- [23] Petrov, A. A., Amirov, R. H. & Samoylov, I. S. On the nature of copper cathode erosion in negative corona discharge. *IEEE Trans. Plasma Sci.* (2009). doi:10.1109/TPS.2009.2018561
- [24] Asinovskii, É. I., Petrov, A. A. & Samoylov, I. S. Erosion of a copper cathode in a negative corona discharge. *Tech. Phys.* (2008). doi:10.1134/s1063784208020230
- [25] Weissler, G. L. Positive and negative point-to-plane corona in pure and impure hydrogen, nitrogen, and argon. *Phys. Rev.* (1943). doi:10.1103/PhysRev.63.96
- [26] Islamov, R. S. & Krishtafovich, Y. A. Lifetime and erosion of silver-based wire electrodes in an ultracorona in air. *J. Electrostat.* (2013). doi:10.1016/j.elstat.2012.12.019
- [27] Islamov, R. S. & Krishtafovich, Y. A. Erosion and lifetime of tungsten, gold, and Nichrome wire anodes in an Ultracorona in air. *IEEE Trans. Plasma Sci.* (2013). doi:10.1109/TPS.2013.2263513
- [28] Puago, H. CEDRION C.T.I S. L, Spanish Patent No. P20183032.
- [29] Selivonin, I. V., Lazukin, A. V., Moralev, I. A. & Krivov, S. A. Effect of electrode degradation on the electrical characteristics of surface dielectric barrier discharge. *Plasma Sources Sci. Technol.* (2018). doi:10.1088/1361-6595/aacbf5
- [30] Wen, T. Y. & Su, J. L. Corona discharge characteristics of cylindrical electrodes in a two-stage electrostatic precipitator. *Heliyon* (2020). doi:10.1016/j.heliyon.2020.e03334
- [31] Limon, S., Yadav, O. P. & Liao, H. A literature review on planning and analysis of accelerated testing for reliability assessment. *Qual. Reliab. Eng. Int.* (2017). doi:10.1002/qre.2195
- [32] Cifuentes, S. C., Monge, M. A. & Pérez, P. On the oxidation mechanism of pure tungsten in the temperature range 600-800°C. *Corros. Sci.* (2012). doi:10.1016/j.corsci.2011.12.027

- [33] Aguirre, M. V. *et al.* Mechanical properties of tungsten alloys with Y₂O₃ and titanium additions. in *Journal of Nuclear Materials* (2011).
doi:10.1016/j.jnucmat.2010.12.120

Figures

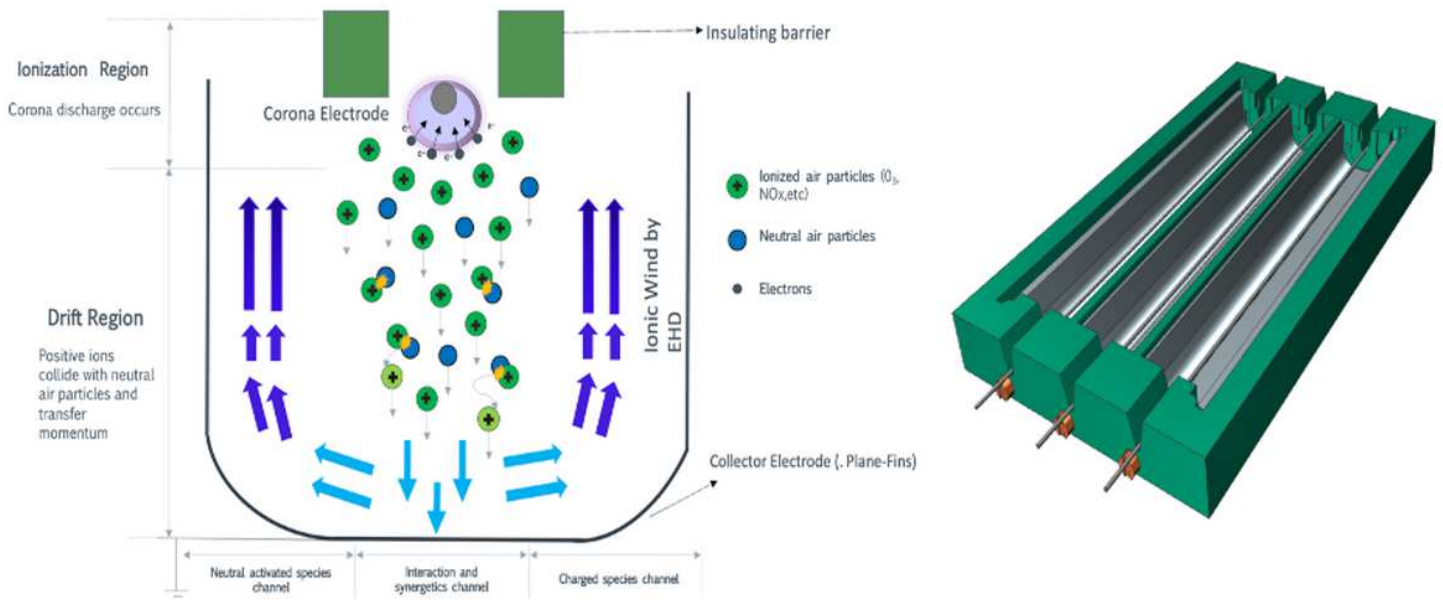


Figure 1

Schematic diagram of positive corona discharge and CAD design of TRAIID configuration.

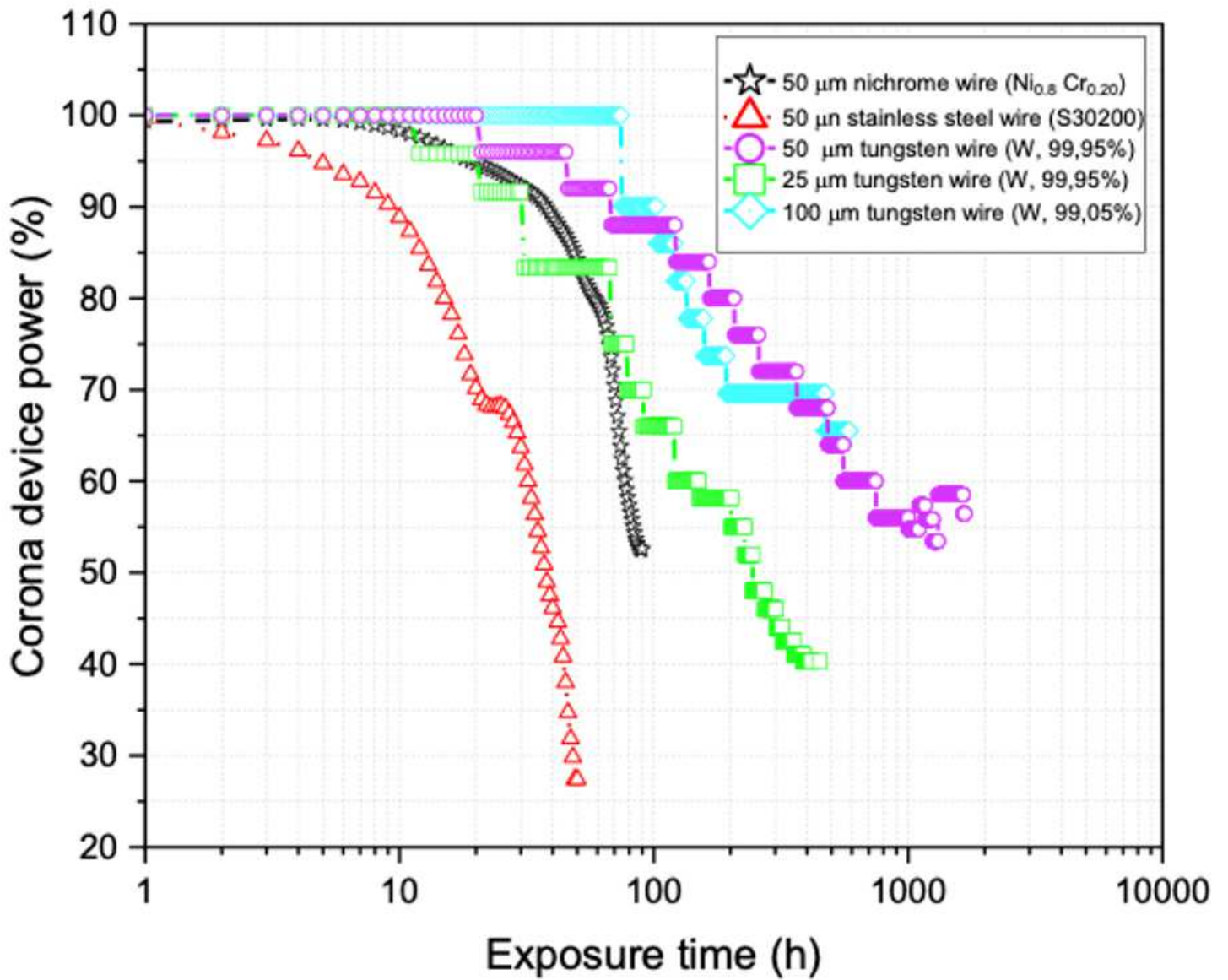


Figure 2

Power loss of different electrode wires under positive high voltage corona discharge.

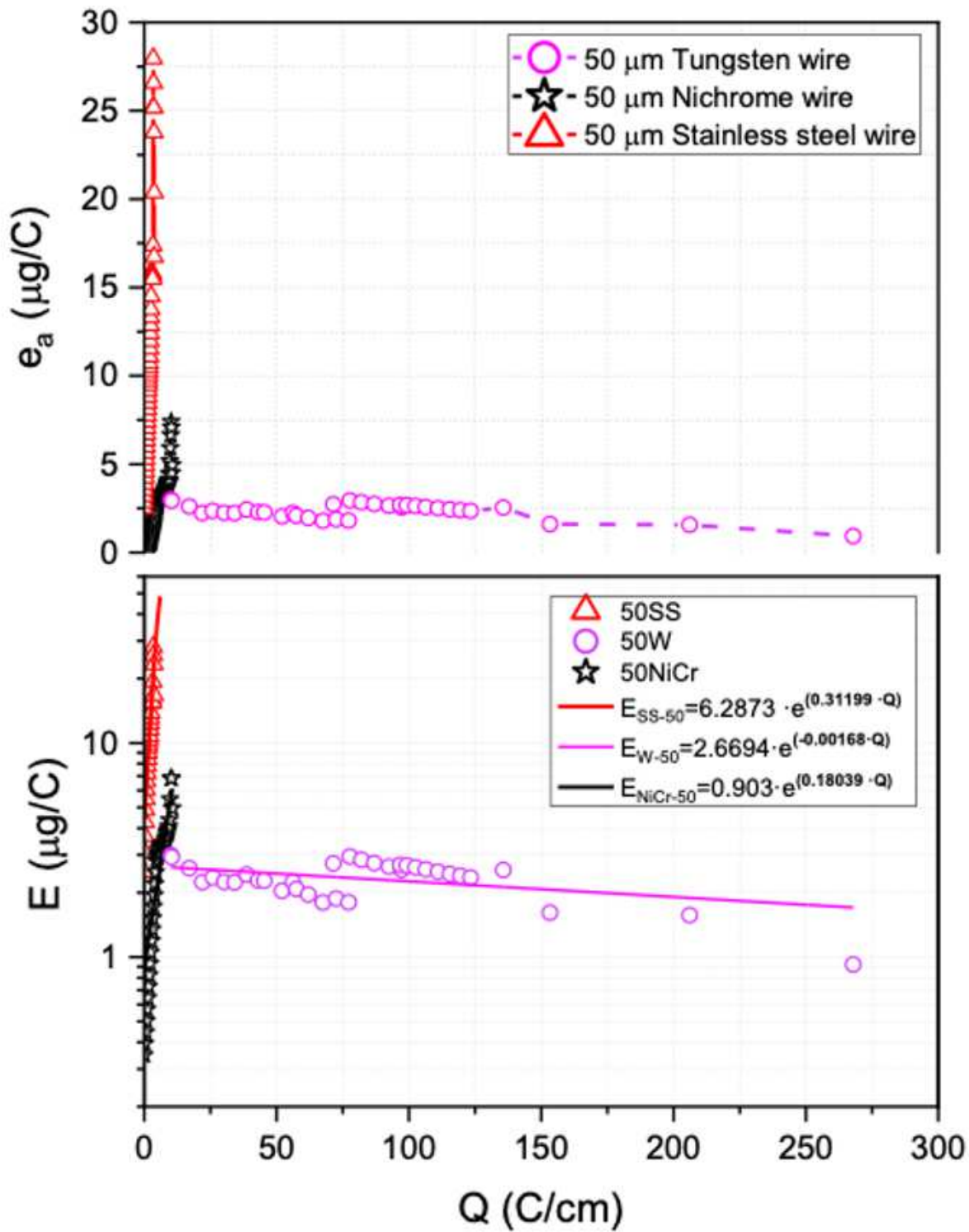


Figure 3

Analysis of tungsten, nichrome and stainless steel as corona electrodes relating average erosion rate (e_a) and erosion rate (E) depending on transferred charge. All corona electrode assays are shown in Table 1.

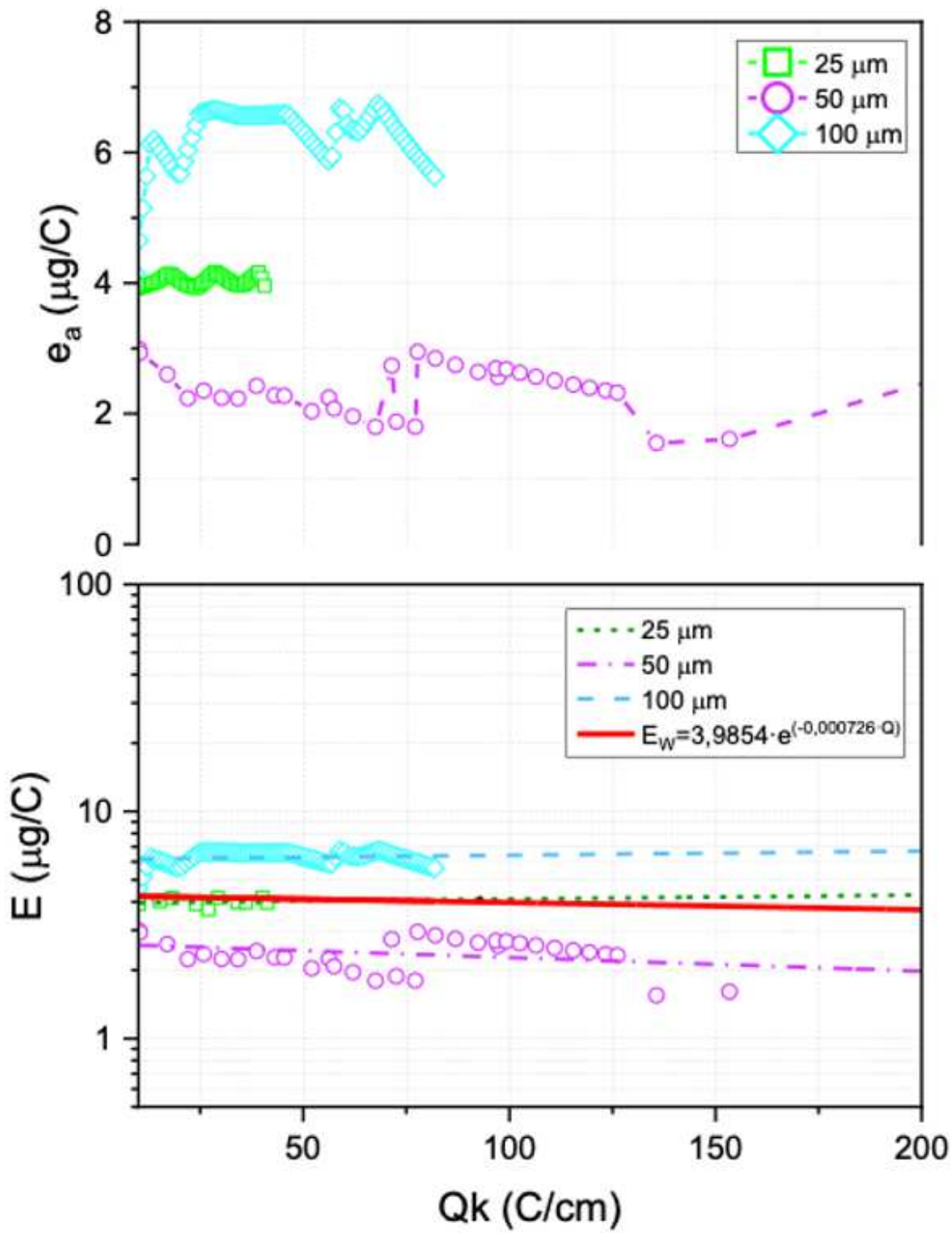


Figure 4

Average erosion rate and global erosion rate S depends on charge transferred per unit length Q considering different tungsten wire diameters.

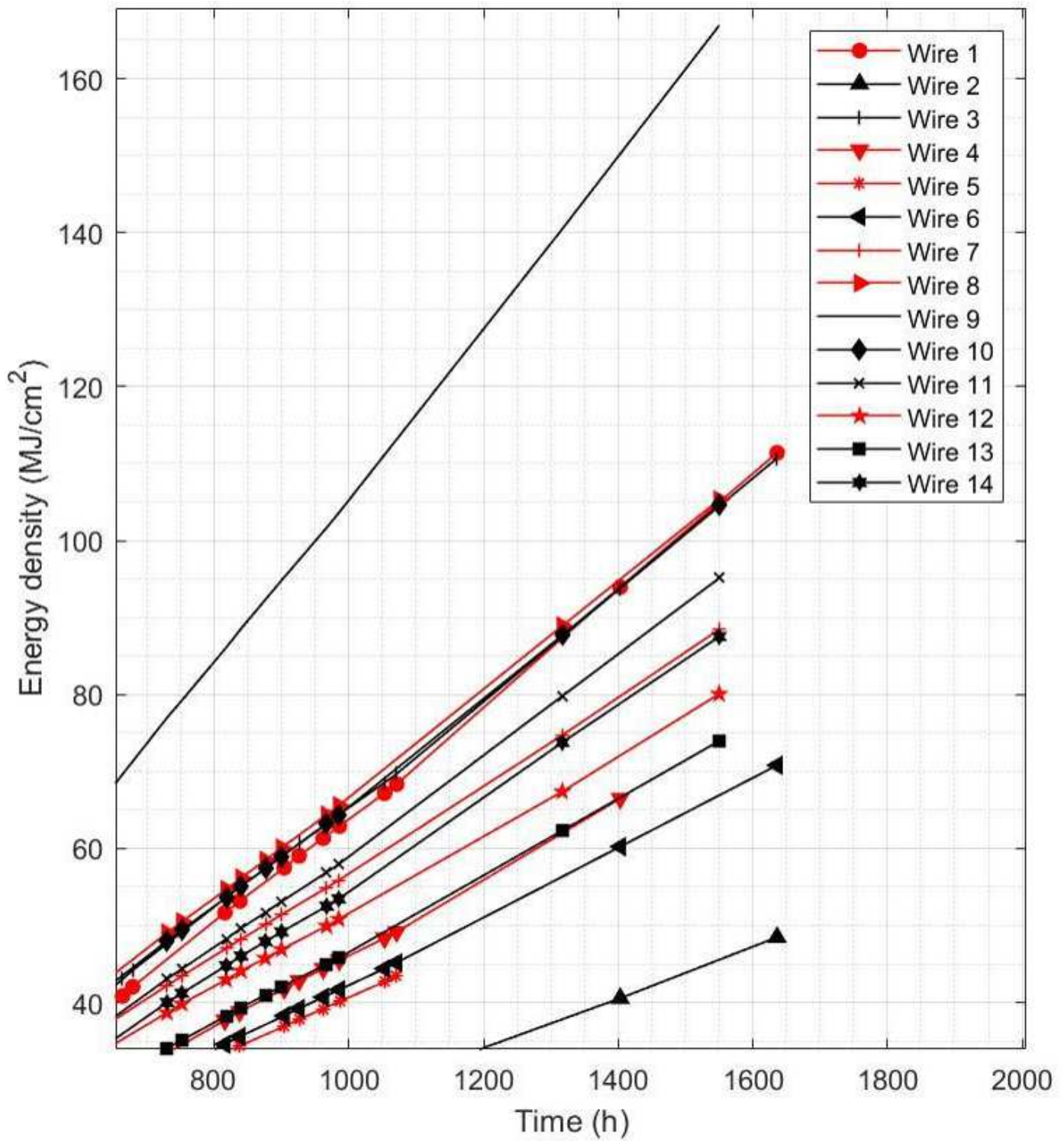


Figure 5

Cumulated energy density (MJ/cm²) recorded for 14 wire electrodes tested for 1,550-1,630 hours.

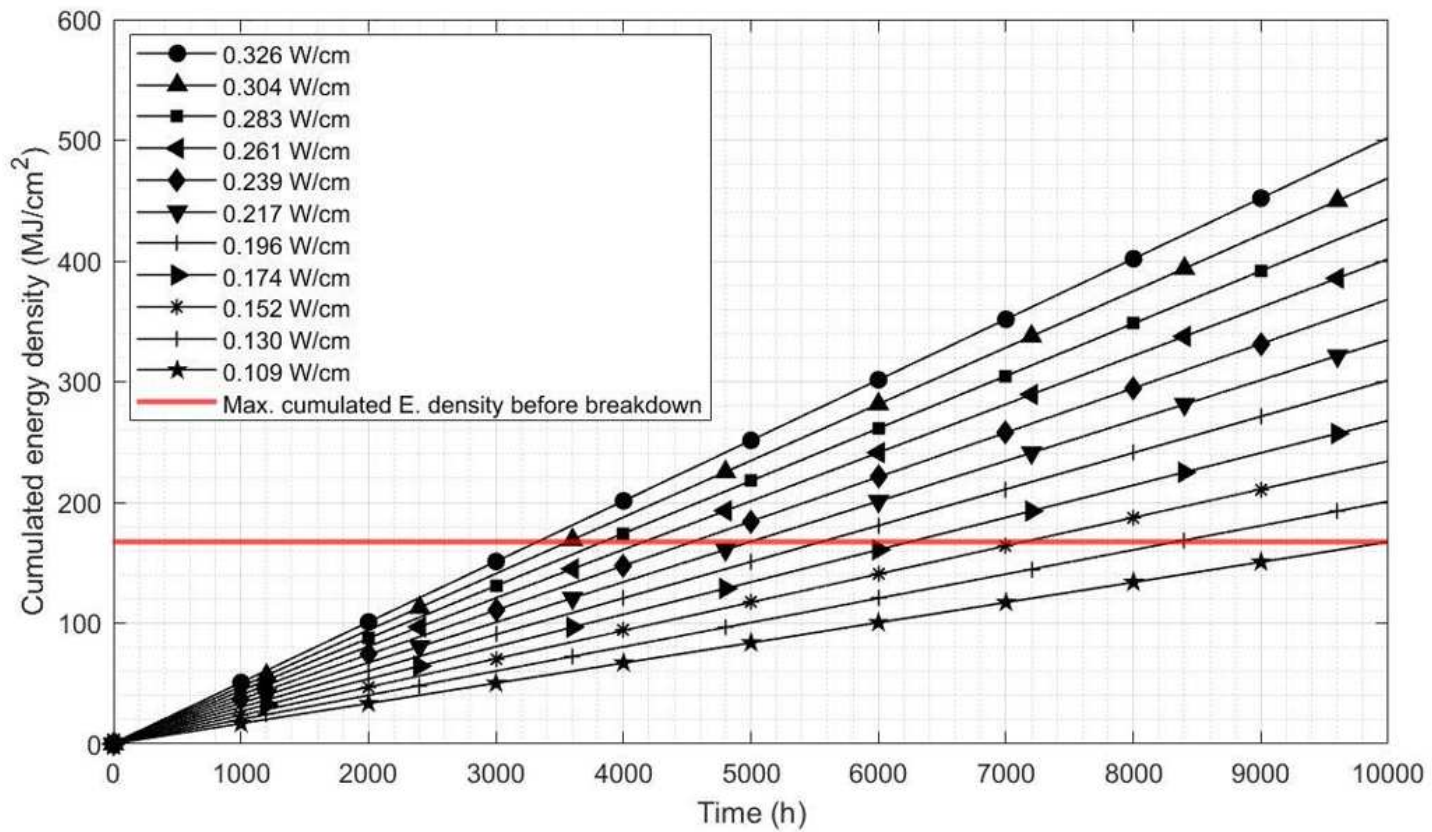


Figure 6

Service life prediction for different levels of power density on wire electrodes.

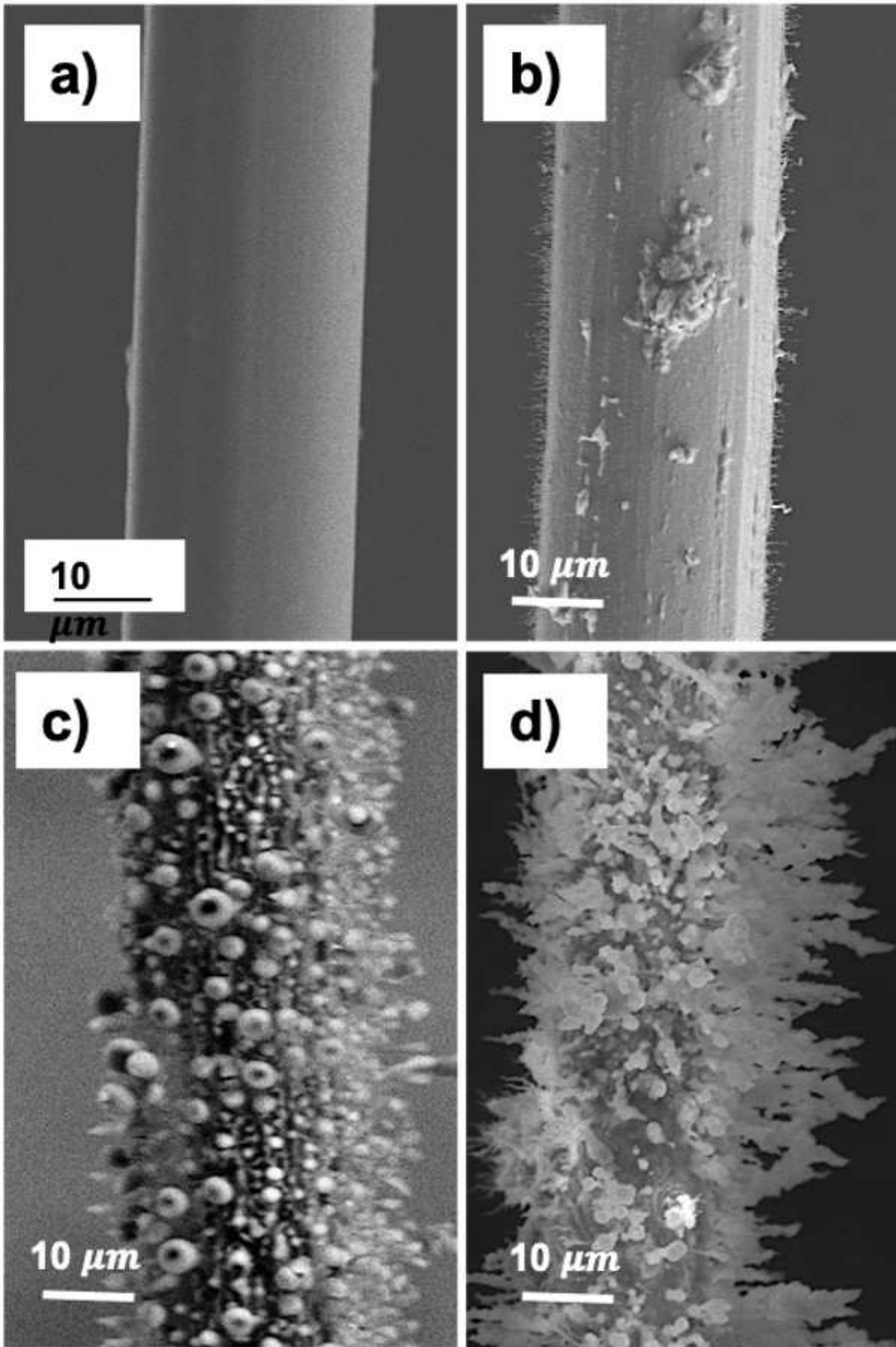


Figure 7

Tungsten wire of 25 μm exposed at a) 0 hours, b) 20 hours, c) 280 hours and d) 450 hours by atmospheric corona discharge.

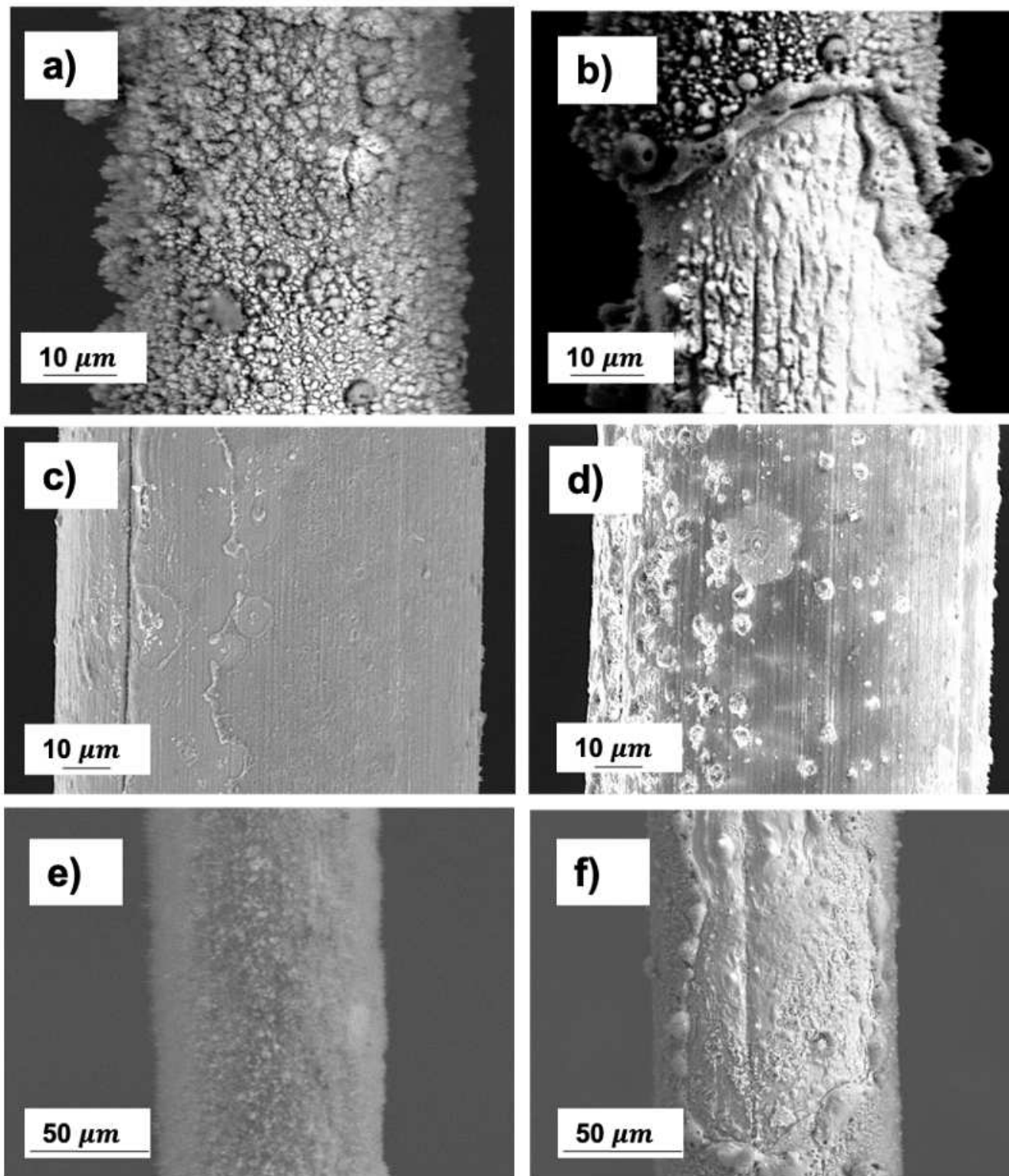


Figure 8

Tungsten filament of 50 μm after treatment at a) and b) 250 hours which a dense and non-uniform oxidation layer can be observed on the entire external surface, observing in some areas the rupture of the oxide layer due to the instability of the discharge. In the micrographs c) and d), the 100 microns tungsten anode is visualized at different exposure hours, 40, 180 hours respectively, where bombardments begin to occur by the electrons. e) and f) SEM images showing W filament of 100 μm undergoes a corona

discharge at 470 hours, showing stable layer of oxides with a pattern similar to velvet and fused areas due to the generation of punctual micro-arcs.

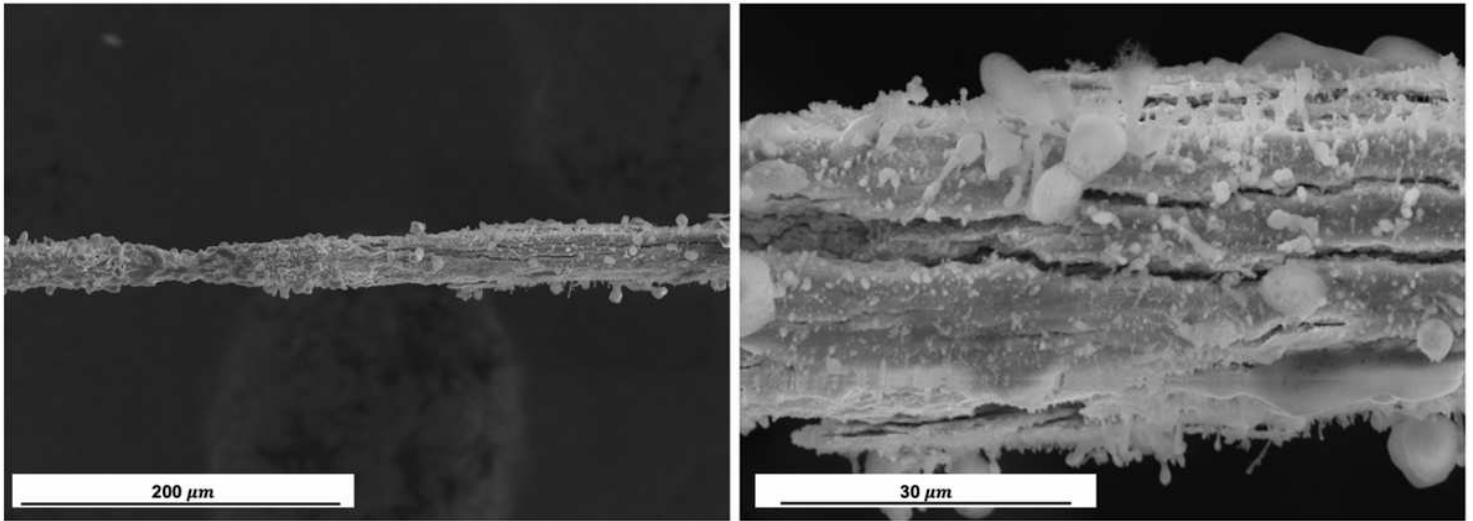


Figure 9

Thickness change of W wire of 25 μm after 300 hours in service due to erosion and corrosion triggered in the process. There is a reduction in section that may be due to the combination of localized detachment by micro-arcs. Also due to plastic deformation favored by focused temperature increases in specific arc-areas. Necking has been observed in some filaments without appreciable degradation.